

Journal of Materials Chemistry A

Accepted Manuscript



This is an *Accepted Manuscript*, which has been through the Royal Society of Chemistry peer review process and has been accepted for publication.

Accepted Manuscripts are published online shortly after acceptance, before technical editing, formatting and proof reading. Using this free service, authors can make their results available to the community, in citable form, before we publish the edited article. We will replace this *Accepted Manuscript* with the edited and formatted *Advance Article* as soon as it is available.

You can find more information about *Accepted Manuscripts* in the [Information for Authors](#).

Please note that technical editing may introduce minor changes to the text and/or graphics, which may alter content. The journal's standard [Terms & Conditions](#) and the [Ethical guidelines](#) still apply. In no event shall the Royal Society of Chemistry be held responsible for any errors or omissions in this *Accepted Manuscript* or any consequences arising from the use of any information it contains.

Cite this: DOI: 10.1039/c0xx00000x

PAPER

www.rsc.org/ees

Porous Carbon Nanotubes Etched by Water Steam for High-Rate Large-Capacity Lithium-Sulfur Batteries

Zhubing Xiao,[‡] Zhi Yang,^{**} Huagui Nie, Yanqi Lu, Keqin Yang, Shaoming Huang*

Received (in XXX, XXX) Xth XXXXXXXXX 20XX, Accepted Xth XXXXXXXXX 20XX

DOI: 10.1039/b000000x

The current investigation of lithium-sulfur (Li-S) batteries faces three practical problems: (1) the poor conductivity of sulfur; (2) the notorious shuttle mechanism; and (3) the volume variation of the sulfur cathode. In principle, carbon nanotubes (CNTs) have high potential in improving sulfur usage because of their high electrical conductivity. Furthermore, opening holes in CNTs or creating pores on the walls is also a useful approach to not only enhance the diffusion of Li ion, but enable more sulfur to fill the interior of the CNTs, which would be beneficial in retaining the soluble poly-sulfide intermediates and accommodate volume variations. Herein, we designed a mild one-step oxidation approach to create porous CNTs (PCNTs) through the chemical reaction between CNTs and the rare oxygen sourced from nebulized water stream at high temperatures. Higher specific surface area and pore volume values confirmed that PCNTs had significant porosity, compared with raw CNTs. When the PCNTs/S composites was tested as cathode in Li-S batteries, the cathode with 78 wt% S content exhibited an initial reversible capacity of 1382 mA h g⁻¹ at 0.2 C. Furthermore, a reversible capacity of 150 mA h g⁻¹ can be preserved even at a very high current rate of 15 C. More importantly, it is also confirmed that a cathode with 89 wt % S content unexpectedly delivered a reversible capacity as high as 1165 mA h g⁻¹ sulfur/830 mA h g⁻¹ electrode at the initial cycle, and 792 mA h g⁻¹ sulfur/564 mA h g⁻¹ electrode after 200 cycles at a current rate of 0.2 C. To the best of our knowledge, such a high rate performance (15 C) and S loading (89 wt %) in cathodes of advanced Li-S batteries have been infrequently reported in previous researches.

1. Introduction

In recent years, because of their lighter weight, longer life, and higher capacity compared to other rechargeable batteries, lithium-ion batteries have been extensively used as the primary electrical energy storage device in various portable electronics.^[1] However, the present energy densities of such batteries are reaching their limit, making it difficult to meet the ever-increasing demand of key markets, such as electric vehicles, in the long term. Searching for the next generation batteries with high energy density and lower cost is urgent. Because of the high theoretical energy density (2567 Wh Kg⁻¹) and specific capacity (S: 1675 mA h g⁻¹), competitive cost and environmental benignity, lithium-sulfur (Li-S) batteries have been widely considered as an appealing candidate for the next generation of large-scale and high-energy storage devices.^[2, 3] However, the current investigation of Li-S batteries still faces three practical problems: (1) the intrinsic poor electronic conductivity of sulfur; (2) the high solubility of the poly-sulfide reaction intermediates (Li₂S_n,

4 < n < 8) and their notorious shuttle mechanism in organic electrolytes; and (3) the volume variation of the sulfur cathode during cycling.^[4, 5]

To overcome these critical issues, one popular approach is to confine the sulfur in a multifunctional carbon matrix, which would improve the electrical conductivity of the S cathode, trap the soluble poly-sulfide intermediates, and accommodate the volume variation of the S cathode. Recently, many types of carbon materials such as ordered mesoporous carbon,^[6] hierarchical porous carbon,^[7] hollow carbon spheres,^[4, 5, 8] and graphene^[9] have been developed as the confining/conductive medium and have produced improved performances in Li-S battery applications. However, the synthesis of these carbon materials or carbon-sulfur composites typically requires high cost and extensive procedures involving multiple surface coatings followed by partial dissolution of S,^[7] or the use of corrosive acids to remove templates.^[5] Obviously, these complex designs and fabrication processes are ill-suited for large-scale practical applications of Li-S batteries. With the rapid progress in industrial mass production and commercialization of carbon nanotubes (CNTs),^[10] the incorporation of S into CNTs for advanced Li-S batteries may be one of the more promising options. Furthermore, in principle, CNTs have high potential in improving sulfur usage and restraining the solubility of lithium poly-sulfides because of their high degree of graphitization, electrical conductivity, and excellent mechanical properties.^[11] Recently, some researchers have attempted to fabricate CNTs/S

Nanomaterials and Chemistry Key Laboratory, Wenzhou University Wenzhou, 325027 (P. R. China).

E-mail: yang201079@126.com, smhuang@wzu.edu.cn,

Fax: (+86)577-8837-3064

† Electronic Supplementary Information (ESI) available: TEM, SEM, XRD, XPS, IR, TGA, Nitrogen sorption isotherms and electrochemical properties of these samples are given.

‡ Z. Xiao and Z. Yang contributed equally to this work

cathodes that achieve high specific capacities exceeding 1200 mA h g^{-1} corresponding to the initial charging capacity.^[12, 13] However, the relatively high decay rates and low sulfur loading and content in these CNTs/S cathodes remain tricky problems.

This may originate from the relatively low specific surface area (SSA) ($<250 \text{ m}^2 \text{ g}^{-1}$) and specific pore volume (V_T) ($<1 \text{ cm}^3 \text{ g}^{-1}$) of the common CNTs, as well as the weak interface bonding between S and the CNT matrix, thus limiting the capturing of sulfur and retaining of soluble poly-sulfides. Opening holes in CNTs or creating pores on the walls is the ideal approach to further increase SSA and V_T of CNTs. Furthermore, porous walls will not only enhance the diffusion of Li^+ in the electrolyte, but enable more sulfur to fill the interior of the CNTs, which would be beneficial in retaining the soluble poly-sulfide intermediates and accommodate volume variations. Although some recent treatments involving chemical oxidation using strong acid or alkali, or electron irradiation, to create pores in CNTs have been confirmed,^[15-16] the structural integrity and high electrical conductivity of the nanotubes cannot be retained, owing to the harsh reaction conditions. Therefore, for advanced Li-S batteries, a milder oxidation treatment is highly desired to make CNTs porous while retaining its structure and electrical conductivity.

It is well known that water is a natural greenest solvent. When water is heated to approximately $1000 \text{ }^\circ\text{C}$, a small percentage is separated into oxygen and hydrogen. Inspired by this fact, we designed a mild one-step oxidation approach to create porous CNTs (PCNTs) through the chemical reaction between CNT and the rare oxygen sourced from nebulized water stream at high temperatures. Higher SSA and V_T values confirmed that CNTs etched by water steam had significant porosity compared with raw CNTs. The milder method holds several advantages: (1) pore size was easy to control, (2) structural integrity and high electrical conductivity of CNTs were retained, (3) no rudimental outgrowths were developed, and (4) oxygen-containing groups in PCNTs were introduced in abundance. When etched PCNTs/S composites were tested as the cathode material in Li-S batteries, the cathode exhibited a high reversible capacity, excellent rate performance, and good cycle stability. The simplicity, greenness, and scalability of this method mean a potential boost in the near future to produce PCNTs with high SSA and V_T for real applications in advanced Li-S battery.

2. Results and discussion

The preparation of etched PCNTs is illustrated in Figure 1. In a typical procedure, water is first nebulized to create a mist of droplets. The droplets formed are then passed into a quartz tube of raw commercial CNTs using an Ar-carrying gas when the desired temperature of $850 \text{ }^\circ\text{C}$ is reached. The final product is then collected from the quartz tube. The morphological structures of the obtained PCNTs samples (Figures 2a and S1) were observed by transmission electron microscopy (TEM), which reveals that the 850PCNTs exhibit abundant lattice defects and the outer shell and surface appears irregular and rough compared with the raw CNTs. Figure 2b shows the nitrogen sorption isotherm of the as-prepared PCNTs; the isotherm feature

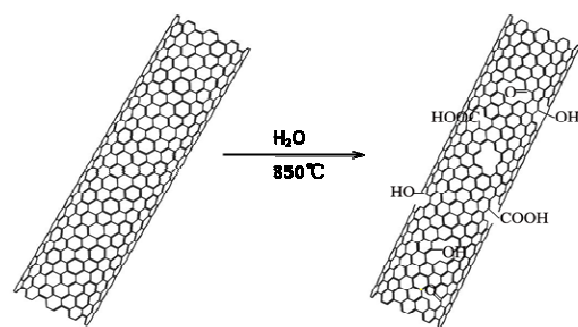


Figure 1 Schematic of the synthesis process of the PCNTs

hysteresis between desorption and adsorption branches indicating the presence of mesopores.^[17] Along with SSA and V_T , the mesopore volume (V_{Meso}) and micropore volume (V_{Micro}) of these PCNT samples etched at various temperatures are summarized in Table 1; values of V_T and SSA of these PCNTs have significantly increased compared with the raw CNT values. The result coupled with TEM observations strongly confirmed that CNTs can be etched by water steam at high temperatures ($750\text{-}950^\circ\text{C}$). It is speculated that the increase of SSA and pore volume of these etched PCNTs may be due to opening some closed structure in the inner cavity of CNTs or creating some pores on the walls.

A clear understanding of the porosity can be deduced through the pore size distribution (PSD) analysis derived from the Barrett-Joyner-Halenda method. The typical PSD curves in Figure 2c and d clearly show the variation in mesopore size ($2\text{-}10 \text{ nm}$) for these CNTs before and after water etching, whereas Table 1 shows that there is little variation in micropore volume in V_T , and the variation in V_{Meso} is dominant in these PCNTs. These data indicate that the mild etching reaction on CNTs have mainly occurred at the mesopore ($2\text{-}10 \text{ nm}$) scale. Furthermore, from Table 1, SSA and V_T are found to gradually increase as the etching temperature changes from 750 to $950 \text{ }^\circ\text{C}$. For the 950PCNTs, the SSA and V_T are $431.2 \text{ m}^2 \text{ g}^{-1}$ and $2.16 \text{ cm}^3 \text{ g}^{-1}$, which are much larger than that of the raw CNTs with $255 \text{ m}^2 \text{ g}^{-1}$ and $0.81 \text{ cm}^3 \text{ g}^{-1}$. With the temperature fixed at $850 \text{ }^\circ\text{C}$, the SSA and V_T also increase with extended etching times. These results suggest that both etching temperature and time should be critical factors in this mild oxidation reaction. It is believed that SSA, V_T , and pore-size distribution for these PCNTs can be controlled by changing these factors.

To clarify whether the PCNTs maintain their intrinsic tubular structures during water etching, measurements from wide-angle-powder X-ray diffractometry (XRD) (Figure S2a) and Raman spectroscopy (Figure S2b) were obtained. From Figure S2a, all PCNTs display two similar peaks (43.4° and 26.2°) corresponding to the (100) and (002) planes, respectively) as for CNTs. In Figure S2b, the intensity ratio I_D/I_G is increased stepwise with the etching temperature increasing. However, this variation occurred in a small scale (i.e., varying from 1.27 to 1.49), which suggests that the water etching only produces a little damage and the intrinsic structure of CNTs is largely reserved.

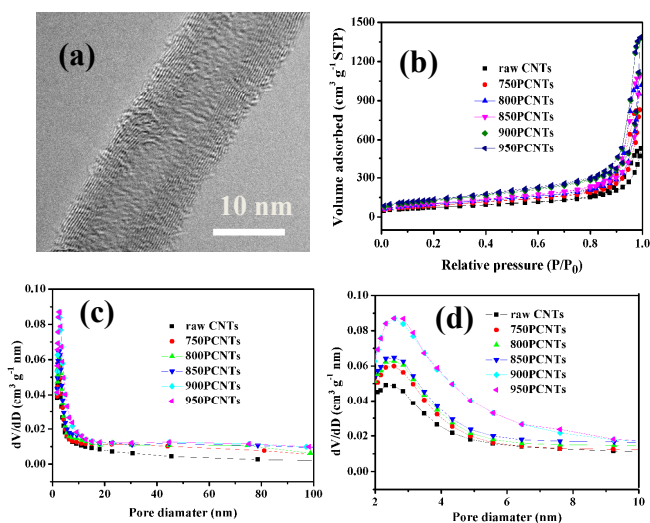


Figure 2 (a) Typical TEM images of the 850PCNTs; (b) Nitrogen sorption isotherms of various PCNTs and raw CNTs; (c, d) pore size distribution of various PCNTs and raw CNTs.

In principle, the large SSA and V_T are acceptable in maintaining excellent electrical properties for these PCNTs, thereby rendering them promising electrode material for energy storage. The performance of PCNTs was evaluated as the sulfur host for Li-S batteries. Typically, the 850PCNT/S nanocomposites (850PCNT-S) are prepared using a melt-diffusion process at 160 °C. After loading with 78wt % S (Figure 3a), no bulk S particles can be found from the scanning electron microscope (SEM) and TEM images (Figures 3b, c, and S3a-d). The corresponding elemental maps (Figure S3e-g) and the line-scan analysis of the hybrids (Figure 3e) demonstrate a uniform distribution of S onto the PCNTs. Furthermore, from the high-resolution TEM images in Figure 3d, S can be observed to have permeated into the interior of the 850PCNTs. In Figure 3f, no characteristic XRD peaks of pure S phase can be detected in the 850PCNT-S nanocomposites, which also indicate a uniform distribution of S particles with small size in the composite cathode. Furthermore, from Figure S4a and b, the 850PCNTs were found to possess a high SSA of 367.2 m² g⁻¹ and large V_T of 1.68 cm³ g⁻¹, which reduced to 5.4 m² g⁻¹ and 0.017 cm³ g⁻¹, respectively, after the incorporation of S, indicating that S filled into most of the pores.

To study the electrochemical properties of the as-made PCNT-S nanocomposites, CR2025 coin cells with metallic lithium anode were fabricated and evaluated. Note that all capacity values stated are given in mA h g⁻¹ per sulfur mass if not mentioned specifically. The kinetic processes of sulfur reduction and sulphide oxidation of the 850PCNT-S composites were studied using cyclic voltammetry. From the results shown in Figure 4a, there are two peaks in the first cathodic reduction process. The peak at 2.32 V (vs Li⁺/Li⁰) corresponds to the reduction of elemental sulphur (S₈) to polysulphide anions (S_x²⁻; 2 < x < 8). A strong cathodic peak at 2.05 V (vs Li⁺/Li⁰) suggests a strong reduction of soluble polysulphide anions to an insoluble low-order Li₂S₂/Li₂S deposit. In the first anodic process, the oxide peak at about 2.35 V is associated with the formation of Li₂S_n (n > 2).^[2, 7] From the second to the fourth cycles, the

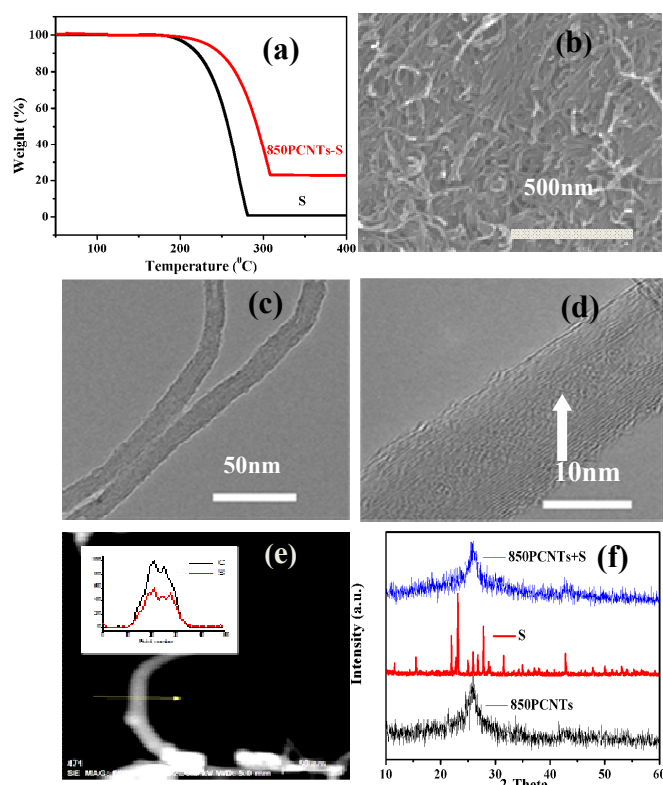


Figure 3 (a) TGA curve of 850PCNT-S composites. Typical SEM (b), TEM (c), HRTEM (d) and line scan analysis (e) images for 850PCNT-S composites. (f) X-Ray diffraction curves of S, 850PCNTs and 850PCNTs-S composites.

potentials of the two reductive peaks exhibit a slight positive shift, whereas the oxide peak gradually shifts to lower potentials, implying that the cell obtains a better reversibility and a more reliable stability for the extended cycles.^[18] Moreover, the variation of oxidation peaks between the first and second cycles may be ascribed to the rearrangement of active sulfur from its original position to more energetically stable sites. Similar phenomenon can also be found in previous report.^[5,18] The charge-discharge curves under various current rate were depicted in Figure S5. Consistent with results from cyclic voltammetry, it can be observed the typical two-plateau behavior of the sulfur cathode, corresponding to the formation of long-chain polysulfides (Li₂S_x, 4 ≤ x ≤ 8) and short-chain Li₂S₂ and Li₂S. Similar to the study elsewhere,^[8] inevitable polarization of the cathode materials is also observed due to fast electron transfer with the increasing current rates. The rate capability of the 850PCNT-S composite at various current densities from 0.5-15 C is shown in Figure 4b. Compared with the raw CNTs/S composite, the 850PCNTs-S composite exhibits a much higher capacity at various rates, with specific capacities of 1308, 985, 922 mA h g⁻¹ at 0.5, 1, and 2 C, respectively. Furthermore, a reversible capacity of 150 mA h g⁻¹ can be preserved even at a very high current rate of 15 C. More importantly, a reversible capacity of 1035 mA h g⁻¹ can still be reversed when the current is switched back to 0.5 C, which is close to the initial capacity (1052 mA h g⁻¹), indicating a highly reversible and excellent rate performance for the 850PCNT-S nanocomposites. To the best of our knowledge to

Table 1 Textural properties of raw CNT and PCNT samples

Samples	Temperatur e(°C)	Time (min)	SSA ^a (m ² g ⁻¹)	V ^b _T (cm ³ g ⁻¹)	V ^c _{Meso} (cm ³ g ⁻¹)	V ^d _{Micro} (cm ³ g ⁻¹)	Average Pore (width/nm) ^e
Raw CNTs			255.3	0.81	0.799	0.011	12.7
750PCNTs	750	10	315.7	1.28	1.273	0.007	16.3
800PCNTs	800	10	349.1	1.56	1.559	0.011	18.3
850PCNTs-1	850	3	320.5	1.31	1.369	0.009	16.7
850PCNTs-2	850	5	341.5	1.52	1.51	0.010	18.0
850PCNTs	850	10	367.2	1.68	1.669	0.011	18.6
850PCNTs-3	850	20	401.9	1.97	1.961	0.009	18.9
A-850PCNTs	850	10 ^f	367.0	1.62	1.614	0.006	18.2
900PCNTs	900	10	421.1	2.10	2.092	0.011	19.2
950PCNTs	950	10	431.2	2.16	2.159	0.011	19.5

a Specific surface area; b Total pore volume; c Mesopore volume; d Micropore volume;

e Average pore size (estimated from the equation of $4Vt/SBET$); f Etched for 10min and kept annealing for 1h in argon

date, such a high rate performance (especially higher than 10 C) for the Li-S battery with 78 wt% S content has only appeared spasmodically possibly because of the intrinsic poor electronic conductivity of sulfur.^[8] The cycling stability of the 850PCNT-S nanocomposite is illustrated in Figure 4c. An initial reversible capacity of 1382 mA h g⁻¹ is achieved at the current rate of 0.2 C, which is about 82.5% of sulfur usage based on the theoretical value (1675 mA h g⁻¹) for sulfur. A rapid capacity drop is seen in the next three cycles followed by good stability on subsequent cycling, which has been explained by an activation step, whereby S in the hybrids is not initially fully accessible to the electrolyte because the pores are filled.^[5] After the first few cycles, about 950 mA h g⁻¹ is achieved over 250 cycles with a steady coulombic efficiency of 93%. In stark contrast, the raw CNT-S composites only remain 171 mA h g⁻¹ after 250 cycles and exhibit

low Coulombic efficiency, which show poor cycling stability. Figure 4d shows the cycling stability of the 850PCNTs-S nanocomposite at some relatively high rates. With a high current rate of 5 C, the capacity remains 455 mA h g⁻¹ after 250 cycles vs 652 mA h g⁻¹ after the first cycle with a capacity fading rate of 0.8 mA h g⁻¹ per cycle. Furthermore, from Figure S6a, no obvious changes can be observed for both the anodic/cathodic peaks in the voltammetric profiles, and there is no evident increase in combination resistance from electrochemical impedance spectroscopy after 200 cycles (Figure S6b), indicating good electrochemical stability for the 850PCNTs-S cathode.

For such an excellent rate performance and high capacity in the 850PCNTs-S cathode, the porous structure in 850PCNTs may be one of the important factors because of their intrinsic capability to trap soluble intermediate poly-sulfides, and to accommodate volume variations of the S cathode. Moreover, the porous structure can also help to convey Li⁺ ions in the electrolyte in consequence of the large number of pores.^[14] In addition, from the IR spectroscopy of the 850PCNTs in Figure S7a, the presence of the oxygen-containing groups (indicated by the strong peak at 3434 cm⁻¹)^[19] is particularly noteworthy. The XPS curve in Figure S7b also supports the result. For the 850PCNT-S composites, a strong interaction between the PCNTs and S is demonstrated by the fact that the S in the PCNT-S nanocomposites exhibits a better thermal stability compared with pure S powders (Figure 3a). Strong C=S stretching and weak C-S stretching are also detected from FT-IR spectrometry at 1220 and 1098 cm⁻¹, respectively, together with S-O-C stretching at 825 cm⁻¹ (Figure S7a).^[19, 20] In the high-resolution O_{1s} spectra of 850CNTs-S (Figure S7d), an obvious up-shift can be observed compared with that of 850CNTs, which suggests the presence of S-O bind in the 850CNTs-S. All these results imply that S has been chemically bonded to the PCNTs. We believe that the strong chemical bond between S and CNT matrix benefits the absorption of more S and trap soluble intermediate poly-sulfides. To further

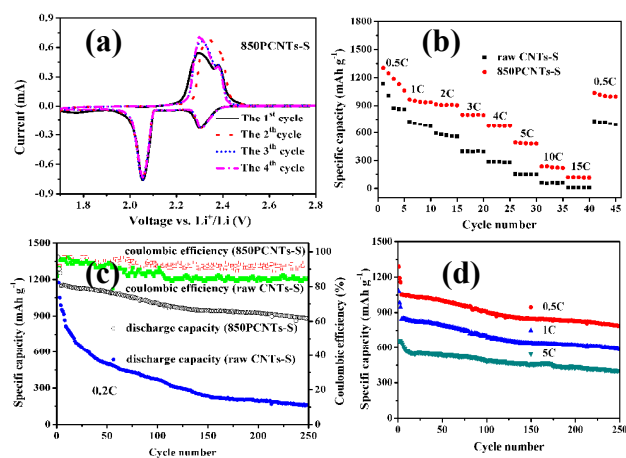


Figure 4 (a) CV profiles of 850PCNTs-S composites; (b) rate performance and (c) cycling stability of raw CNTs-S hybrids and 850PCNTs-S hybrids; (d) cycling stability of 850PCNTs-S composites at various current rate.

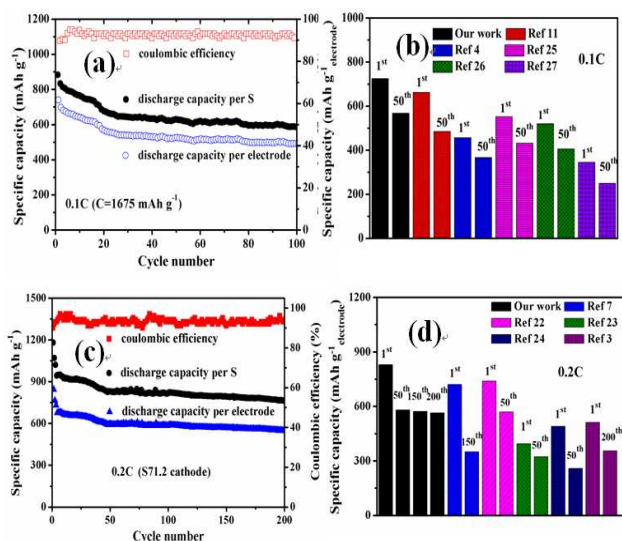


Figure 5 Cycling stabilities and coulombic efficiencies of the S80.1 cathode at a current rate of 0.1C (a), and the S71.2 cathode at a current rate of 0.2C (c); a comparison between our work (the S80.1 (b) and S71.2 (d) cathode) and some other typical reports on the specific capacity per cathode mass

verify the influence of the oxygen-containing groups, the 850PCNTs were annealed at 850 °C in argon for an hour (the obtained material labeled A-850PCNTs), as expected, the peak of hydroxyl groups disappeared (Figure S8). From Figure S9, the as-made A-850PCNT-S cathode is found to exhibit inferior electrochemical performance compared with the 850PCNT-S cathode. Consistent with the voltage profiles (Figure S10), for the A-850PCNT-S composites, the shift in the declining peaks with cycling clearly indicates electrochemical instability. In contrast, the 850PCNT-S composites exhibit narrower peaks with slight shifts with cycling, indicating excellent electrochemical stability. Moreover, for the 850PCNTs-S composites, the difference between the first reduction peak at ~2.32 V and the oxidation peak at 2.35 V is less than that for the A-850PCNT-S composites, suggesting an effective retention of capacity and prevention of the shuttle mechanism. We speculate that the S in the 850PCNT-S composites and the poly-sulfides formed in the redox reaction are not free but bonded to the PCNTs via C-S or S-O-C bonds. The chemically bonded S is slowly converted to free, but highly dispersed, reactive material upon cycling. All these results also strongly confirm that the introduced oxygen-containing groups for the 850PCNTs after water etching should be another important feature for advanced Li-S batteries.

Recent advances involving CNT-S cathodes have demonstrated to enhance the capacity and stability of Li-S batteries. Although in the literature the capacity is reported as very high when calculated only by the weight of S, the specific capacity based on the total electrode mass is generally lower than 500 mA h g⁻¹,^[21] which is mainly attributed to the low content of S (generally lower than 80 wt%). Therefore, to raise the specific capacity of cell-levels in Li-S batteries, the S content in each cell must be increased. Surprisingly, when loaded with 89 wt % of S (Figure S11), the as-prepared 850PCNT-S composite (active material : conductive agent : PVDF = 90 : 5 : 5, i.e., the total content of S in the electrode is 80.1 wt%, dubbed as S80.1)

unexpectedly delivered a reversible capacity as high as 895 mA h g⁻¹_{sulfur}/717 mA h g⁻¹_{electrode} after the initial cycle and 625 mA h g⁻¹_{sulfur}/500 mA h g⁻¹_{electrode} after 100 cycles with a stable Coulombic efficiency of 95% at a low current rate of 0.1 C (Figure 5a). Moreover, when increasing the amount of conductive agent (active material: conductive agent: PVDF = 80 : 10 : 10, i.e., the total content of S in the electrode is 71.2%, dubbed as S71.2), an initial reversible capacity of 1165 mA h g⁻¹_{sulfur}/830 mA h g⁻¹_{electrode} could be obtained at a current rate of 0.2 C. More importantly, 564 mA h g⁻¹_{electrode} could also be retained after 200 cycles, with coulombic efficiencies averaging 95% (Figure 5c). The voltage profiles of the first, 50th, 100th, 150th, 200th cycles were depicted in Figure S12. It can be found that the hysteresis between the charge and discharge cycles increases slightly after 200 cycles, which indicates a good electrochemical stability. Furthermore, even at a current rate of 1 C, a satisfactory capacity of 672 mA h g⁻¹_{sulfur}/478 mA h g⁻¹_{electrode} was achieved, and the recovery of a reversible capacity of 930 mA h g⁻¹_{sulfur}/662 mA h g⁻¹_{electrode} was achieved at 0.2 C following the charge/discharge process at a current rate of 1 C (Figure S13). To the best of our knowledge, these reversible capacity values in our experiments are comparable with those of Li-S batteries given in some recent reports (Figure 5b, d).^[3, 4, 7, 11, 22-27]

3. Conclusions

In summary, we have developed a simple, green, scalable one-step approach to obtain PCNTs with high SSA and V_T, using a mild chemical reaction between CNTs and rare oxygen sourced from nebulized water vapor at high temperatures. We obtained SSA and V_T values for PCNTs after water etching as high as 431.2 m² g⁻¹ and 2.16 cm³ g⁻¹, which are much larger than those for raw CNTs of 255 m² g⁻¹ and 0.81 cm³ g⁻¹. When the etched PCNTs/S composites was tested as cathode material in Li-S batteries, a cathode containing 78 wt % S delivered a high initial capacity of 1382 mA h g⁻¹ and maintained a reversible capacity of 950 mA h g⁻¹ after 250 cycles at a current rate of 0.2 C. Furthermore, the etched CNTs/S cathode also exhibited a good rate performance, and a reversible capacity of 150 mA h g⁻¹ can be preserved at the very high current rate of 15 C. More importantly, we also developed a Li-S battery with higher sulfur content. A cathode with 89 wt % S content unexpectedly delivered a reversible capacity as high as 1165 mA h g⁻¹_{sulfur}/830 mA h g⁻¹_{electrode} at the initial cycle, and 792 mA h g⁻¹_{sulfur}/564 mA h g⁻¹_{electrode} after 200 cycles at a current rate of 0.2 C. To the best of our knowledge, such a high rate performance (15 C) and S loading (89 wt %) in cathodes of advanced Li-S batteries have been infrequently reported in previous researches. PCNTs etched with nebulized water hold great potential for real applications in advanced Li-S batteries. We believe that the mild oxidation treatment can also be applied to prepare other porous graphite materials for catalytic, electronic, and even optical applications.

4. Experimental section

Synthesis of porous carbon nanotube (PCNTs)

The raw carbon nanotubes (dubbed as raw CNTs) for the study were purchased from commercial corporation. In a typical procedure, water was first nebulized to create a mist of droplets.

The droplets formed were then passed into a quartz tube of raw commercial CNTs using an Ar-carrying gas when the desired temperature of 850 °C is reached. After the water etching, the water steams were turned off, and the furnace was cooled to room temperature under argon flow. As a control experiment, other carbon materials obtained under various conditions such as the etching temperature and time were synthesized in the same way. The resulted materials were denoted accordingly as 850PCNTs, 900PCNTs, 850PCNTs-1, 850PCNTs-2, 850PCNTs-3, and so on.

Synthesis of CNTs/Sulfur Composites

The CNTs/S composites were prepared following a melt-diffusion strategy. In a typical procedure, the PCNTs and sulfur (high purity sulfur, 99.99% metal basis, Aladdin) were mixed. Then the powder were ground and heated in an oven at 160°C for 12 h, followed by another 12 h at 180°C. For comparison, the raw CNTs-S composite were prepared via the same method.

Structure Characterization

X-ray photoelectron spectroscopy (XPS) measurements were carried out with an ultrahigh vacuum setup, equipped with a monochromatic Al KR X-ray source and a high resolution Gammadata-Scienta SES 2002 analyzer. X-ray diffraction patterns (XRD) were obtained with a D/MAX-2400 diffractometer using Cu K α radiation (40 kV, 100 mA, $\lambda=1.54056$ Å). Raman spectra were taken under ambient conditions using a Renishaw (inVia) with an Ar-ion laser beam at an excitation wavelength of 532 nm. The nitrogen adsorption/desorption data were recorded at the liquid nitrogen temperature (77 K) using a Micromeritics ASAP 2020 M apparatus. The samples were degassed at 120 °C under vacuum for 3 h prior to the measurement. Pore size distribution (PSD) was derived from the adsorption branch of the isotherms using the Barrett–Joyner–Halenda (BJH) model. Total pore volumes were calculated from the amount adsorbed at a relative pressure (P/P₀) of 0.99. The specific surface area was calculated using the Brunauer-Emmett-Teller (BET) equation. The IR spectrum was collected on a Nicolet 6700 FTIR spectrometer. SEM images were obtained with a JSM-6700F field-emission scan electron microscope. TEM analyses were carried out with a JEOL-3010 instrument operating at 200 kV. The samples for TEM analysis were prepared by dropping dehydrated alcohol droplet of the products on copper grids and drying at 45 °C. Thermo gravimetric analysis (TGA) was measured at a heating rate of 10 °C min⁻¹ under nitrogen flow, using a STA449 F3 Jupiter thermo gravimetric analyzer (NETZSCH).

Electrochemical Characterization

Electrochemical experiments were performed via CR2025 coin-type test cells assembled in an argon-filled glovebox with lithium metal as the counter and reference electrodes at room temperature. The cathode for Li–S batteries was prepared by mixing 90 wt % composite materials, 5 wt % conductive agent and 5 wt % polyvinylidene difluoride (PVDF) in N-methyl-2-pyrrolidone (NMP) to form a slurry. Subsequently, the slurry was pasted onto an aluminum foil after drying at 60 °C overnight and Celgard 2400 membrane was used as the separator to isolate electrons. The electrolyte was 1 M bis(trifluoromethane)

sulfonimide lithium salt (LiTFSI) with 1% LiNO₃ dissolved in a mixture of 1,3-dioxolane (DOL) and dimethoxymethane (DME) (1:1 by volume). The discharge/charge measurements were conducted at a voltage interval of 1.0 to 3.0 V using a CT2001A battery test system (LAND Electronic Co.). Cyclic voltammetry (CV) measurements were performed on CHI6600 electrochemical workstation at a scan rate of 0.2 mV s⁻¹.

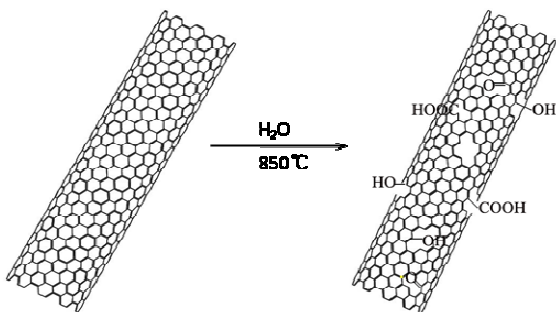
Acknowledgements

The work was supported in part by grants from NSFC (21273163, 51002106, 21005055, 21173259) and NSFC for Distinguished Young Scholars (51025207), ZJST (2012R10014-08), NSFZJ (LY13B050002).

Notes and references

- [1] J.M. Tarascon, M. Armand, *Nature* 2001, **414**, 359.
- [2] H. Chen, W. Dong, J. Ge, C. Wang, X. Wu, W. Lu, L. Chen, *Sci. Rep.*, 2013, **3**, 1910.
- [3] W. Zhou, Y. Yu, H. Chen, F. J. Disalvo, H. D. Abruña, *J. Am. Chem. Soc.*, 2013, **135**, 16736.
- [4] C. Zhang, H. Wu, C. Yuan, Z. Guo, X. Lou, *Angew.Chem., Int. Ed.* **2012**, **51**, 9592.
- [5] G. He, S. Evers, X. Liang, M. Cuisinier, A. Garsuch, L. F. Nazar, *ACS Nano*. 2013, **7**, 10920.
- [6] X. Ji, K. T. Lee, L. F. Nazar, *Nat. Mater.* 2009, **8**, 500.
- [7] D. Li, F. Han, S. Wang, F. Cheng, Q. Sun, W. Li. *ACS Appl. Mater. Inter.*, 2013, **5**, 2208.
- [8] N. Brun, K. Sakaushi, L. Yu, L. Giebeler, J. Eckert, M. M. Titirici, *Phys. Chem. Chem. Phys.* 2013, **15**, 6080.
- [9] C. Zu, A. Manthiram, *Adv. Energy. Mater.*, 2013, **3**, 1008.
- [10] Q. Zhang, J. Q. Huang, M. Q. Zhao, W. Z. Qian, F. Wei, *Chem. Sus. Chem.*, 2011, **4**, 864.
- [11] L. Yin, J. Wang, F. Lin, J. Yang, Y. Nuli, *Energy Environ. Sci.* 2012, **5**, 6966.
- [12] S. Dorfler, M. Hagen, H. Althues, J. Tubke, S. Kaskel, M. J. Hoffmann. *Chem. Commun.*, 2012, **48**, 4097.
- [13] J. Huang, Q. Zhang, S. Zhang, X. Liu, W. Zhu, W. Qian, F. Wei, *Carbon* 2013, **58**, 99.
- [14] H. S. Oktaviano, K. Yamadab, K. Waki, *J. Mater. Chem.*, 2012, **22**, 25167.
- [15] J.Y. Eom, H.S. Kwon, *Mater. Chem. Phys.*, 2011, **126**, 108.
- [16] H. Ye, Y. Yin, Sen. Xin, Y. Guo, *J. Mater. Chem. A*. 2013, **1**, 6602.
- [17] P. S. Spinney, D. G. Howitt, S. D. Collins, R. L. Smith, *Nanotechnology*. 2009, **20**, 465301.
- [18] Y. Fu, Y.S. Su, A. Manthiram, *Angew. Chem. Int. Ed.*, 2013, **52**, 6930.
- [19] V. M. Litvinov, P. P. De, *Spectroscopy of Rubber and Rubbery Material*, *Smithers Rapra Publishing, London, UK* **2002**.
- [20] J. Coats, *Interpretation of Infrared Spectra, A Practical Approach*, *John Willy&Sons Ltd, Chichester, UK* **2000**.
- [21] M. Song, Y. Zhang, E. J. Cairns, *Nano Lett.*, 2013, **13**, 5891
- [22] B. Ding, C. Yuan, L. Shen, G. Xu, P. Nie, Q. Lai, X. Zhang, *J. Mater. Chem. A*. 2013, **1**, 1096
- [23] Y. Fu and A. Manthiram, *Chem. Mater.*, 2012, **24**, 3081.
- [24] Y. Yang, G. Yu, J. J. Cha, H. Wu, M. Vosgueritchian, Y. Yao, Z. Bao, Y. Cui, *ACS Nano*. 2011, **5**, 9187.
- [25] S. Chen, Y. Zhai, G. Xu, W. Jiang, D. Zhao, J. Li J, L. Huang, S. Sun, *Electrochimica Acta*. 2011, **56**, 9549.
- [26] G. Xu, Y. Xu, J. Fang, X. Peng, F. Fu, L. Huang, J. Li, S. Sun, *ACS Appl. Mater. Inter.*, 2013, **5**, 10782.
- [27] S. Lu, Y. Chen, X. Wu, J. Liu, *Nano Lett.*, 2013, **13**, 2485.

Entry for the Table of Contents



5 A simple, green, scalable one-step approach to obtain porous
CNTs (PCNTs) with high specific surface area and pore volume
has been developed through a mild chemical reaction between
CNTs and rare oxygen sourced from nebulized water vapor at
high temperatures. When etched PCNTs/S composites were
10 tested as the cathode material in Li-S batteries, the cathode
exhibited a high reversible capacity, excellent rate performance,
and good cycle stability.

15